5.1 ISOTOPE RATIOS OF RAINFALL AND WATER VAPOR OBSERVED IN TYPHOON SHANSHAN

Hironori Fudeyasu[*1], Kimpei Ichiyanagi[1], Atsuko Sugimoto[2], Kei Yoshimura[3], and Manabu D. Yamanaka[1]
[1]Japan Agency for Marine-Earth Science and Technology, Yokosuka, Japan
[2]Hokkaido University, Sapporo, Japan
[3]The University of Tokyo, Tokyo, Japan

1. Introduction

The intensification of tropical cyclone (TC) over the ocean has been examined by several studies (e.g., Ooyama 1964, 1969, Charney and Eliassen 1964, Rotunno and Emanuel 1987, Montgomery et al. 2006). The main energy to TC is the water derived from the evaporation from the nearby tropical ocean and/or converging water vapor in the atmospheric boundary layer from environmental moisture surrounding TC. Atmospheric moisture cycling therefore plays a central role in the TC's intensification, yet few observations of the moisture cycling are available.

Stable hydrogen and oxygen isotope ratios ($^2H^1H^{16}O/^1H_2^{16}O$ and $^1H_2^{18}O/^1H_2^{16}O$) are dynamic tracers for the atmospheric moisture cycling because their compositions are physically influenced by complex atmospheric behavior, water vapor advection, condensation, and evaporation. Many observational studies have examined isotopes of precipitation and/or water vapor (e.g., Ichiyanagi et al. 2005). Lawrence and Gedzelman (1996) suggested the use of stable isotope ratios to investigate moisture cycling of TCs. The mean precipitation isotopes in TCs were markedly lower than those in other tropical and summer precipitation (Lawrence 1997, Lawrence and Gedzelman 2003, Lawrence et al. 2004). Lawrence et al. (1998) speculated that the low precipitation isotopes in TCs were resulted from their high thick clouds, large precipitation region and relative longevity. At the surface over land, the isotope ratios of both precipitation and water vapor in TCs decreased radially inward to the eye (Lawrence and Gedzelman 1996, Lawrence et al. 1998, 2002). The inward decreases in isotope ratios of precipitation and water vapor in TCs may be caused by two factors: (1) inward increased precipitation efficiency due to higher cloud tops and (2) evaporation and diffusive isotope exchange between the falling precipitation and the ambient water vapor. Precipitation becomes enriched in the heavy isotopes as it falls as a result of evaporation of precipitation because the heavier isotopes are concentrated in water. In contrast, the ambient water vapor was isotopically depleted by evaporated water vapor from precipitation. Diffusive isotope exchange between the falling precipitation and the water vapor also lowers the isotope ratio of the ambient water vapor near the surface (Miyake et al., 1968). Lawrence et al. (1998) used a two-dimensional microphysical model with isotope physics developed by Gedzelman and Arnold (1994) to simulate idealized TC situations. The model results showed that, through precipitation regions of TC's rainband, the stepwise isotope exchange between falling precipitation and converging water vapor caused inward decrease in water vapor isotope ratios.

In contrast to the surface-based observational results, isotope ratios of precipitation and water vapor collected over the ocean at heights from 600 to 3000 m during flights in Hurricane Faith, 1967, increased in the eyewall to high values (Ehhalt and Östlund 1970). Recently Gedzelman et al. (2003) collected precipitation and water vapor during flights into four hurricanes at flight levels between 850 and 475 hPa and analyzed for their stable isotopes. The lowest isotope ratios occurred in or near regions of stratiform precipitation between about 50 and 250 km from the eye, but isotope ratios increased inward in the eyewall. Two-layer fractionation chamber model results (Gedzelman et al. 2003) showed that sea spray supplied the eyewall with up to 50 percent of its water vapor and was largely responsible for its high isotope ratios.

Although previous isotopic observations provided much information, there is no surface-based isotopic observational result supporting the increase in the isotope ratios in the eyewall presented by aircraft data (Ehhalt and Östlund 1970, Gedzelman et al. 2003). This may occur because of either coarse temporal interval of the routine observation or difficulty in TC developing over the subtropical sea, or both, in the surface-based isotopic observation. We therefore attempted the intensive surface-based observation with high temporal resolution for the isotopes of both precipitation and water vapor at Ishigaki Island, a small subtropical island, during the passage of Typhoon Shanshan in mid September 2006. Also comprehensive meteorological observations supported the features of the precipitation pattern accompanying Shanshan. These observations lead to a better understanding of

───────────────────────────────
*Corresponding author address: Hironori Fudeyasu, Japan Agency for Marine-Earth Science and Technology, 2-15 Natsushima, Yokosuka, Kanagawa 237-0061 Japan; E-mail: fudeyasuh@jamstec.go.jp

atmosphere moisture cycling in the TC developing over the sea. Moreover we here report the first surface-based measurement for isotope ratios of water vapor in the eye accompanied by a sudden cessation of precipitation.

2. Data and methods

2.1 Isotopic data

Intensive isotopic observation was conducted at Japan International Research Center for Agricultural Sciences (JIRCAS, 24.34ºN, 124.16ºE, 10 m above m.s.l) in Ishigaki Island, southwest of Japan (Fig. 1), from 11 to 18 September 2006. Ishigaki Island is small subtropical island with 221 km^2 in area where is convenient to lead a better understanding of TC developing over the subtropical sea.

Precipitation samples were automatically collected every 1-mm amount of precipitation with an auto-precipitation sampler. Water vapor was cryogenically collected at liquid nitrogen temperature (-196ºC) using an extraction line comprising a U-shape glass tube filled with glass beads (Sugimoto, 2002). Air was introduced from the air inlet on the roof of the building into the extraction line in the laboratory of JIRCAS through polyethylene tube with a vacuum pump equipped at the outlet of the extraction line. Flow rate of the air was reduced to about 150 ml min^{-1} for complete extraction of water vapor. Sampling was continued until at least 0.3 ml of water was obtained, namely, sampling duration depending on the mixing ratio of air sample. It took about 70 minute in our observation. At the end of sampling, carbon dioxide which was trapped with water vapor was vaporized and removed by pumping out at liquid nitrogen ethanol slush temperature (-90ºC). Water vapor samples were collected around 0430, 1030, 1630, and 2230 UTC every day.

Isotopic composition of water samples was analyzed by $CO_2/H_2/H_2O$ equilibration method using mass spectrometer at Graduate School of Environmental Science, Hokkaido University. Isotopic composition are expressed with δ values defined as $\delta_x = (R_x/R_{SMOW} - 1) \times 1000$, where R_x is the isotope ratio in sample, and R_{SMOW} is isotope ratio in standard (standard mean ocean water, SMOW). The δ^2H and $\delta^{18}O$ values of water vapor and precipitation near sea level range from about +40 to -400 per mil and +5 to -50 per mil, respectively (Dansgaard 1964). Analytical errors were less than ±2 per mil for δ^2H and ±0.15 per mil for $\delta^{18}O$, respectively. Deuterium excess (d-excess) was calculated from d-excess=$\delta^2H - 8 \times \delta^{18}O$. The magnitude of d-excess depends on the relative humidity in the evaporation process from sea surface and precipitation (e.g., Craig 1961, Merlivat and Jouzel 1979). The global average value measured in precipitation is 10 per mil.

We also measured the salinity in the collected precipitation by compact electric conductivity meter in order to detect the content of sea spray in precipitation samples. Sea spray, having heavy isotope ratio like ocean water, was trapped together by the falling precipitation, causing the overestimate of precipitation isotope ratios. We therefore corrected the precipitation isotope ratios for content of sea spray, roughly assuming that the isotope content of sea spray is 0 per mil like sea water. The correction equation is written as $\delta_{correct} = \delta_{obs} / (1 - S_{obs} / S_{sea})$, where $\delta_{correct}$ is corrected isotope content in sample, δ_{obs} is isotope content in observed sample, S_{obs} is salinity in observed sample, and S_{sea} is 3.4 percent of salinity in sea water. The isotope content in water vapor samples was not corrected.

2.2 Meteorological data

One-minutes accumulated precipitation and thirty-minute averaged surface pressure, surface wind, temperature, and relative humidity were observed at JIRCAS. Surface wind data averaged over 10-minute intervals derived from the Automated Meteorological Data Acquisition System (AMeDAS) of the Japan Meteorological Agency (JMA) at Ishigaki site was also used. The precipitation pattern over the Ishigaki Island was estimated from operational weather radar map at Ishigaki site provided by the JMA. The echo data have a horizontal resolution of 1.0 km. Precipitation pattern was also derived from the product 2A12 of the Tropical Rainfall Measuring Mission (TRMM) Microwave Imager (TMI). The product 2A12 data consists of instantaneous TRMM precipitation retrievals with a horizontal resolution of about 5.1 km. The equivalent black body temperature (T_{BB}) of satellite images from the Geostationary Meteorological Satellite (MTSAT) were also used in this study. The satellite date has a horizontal resolution of 0.2°.

The track of Shanshan was obtained from the Best Track data of the Regional Specialized Meteorological Centers (RSMC) Tokyo–Typhoon Center. The dataset consists of the names, positions, maximum surface pressure, and maximum wind speeds of TCs, recorded at 3-hour intervals around Ishigaki Island. Estimates of the 10-minutes positions of the cyclone center were determined by the spline interpolation of the 3-hour data.

3. Results

3.1 Precipitation pattern of Typhoon Shanshan

Figure 1 shows the track of Shanshan derived from

the Best Track data. Shanshan was upgraded to a tropical storm (maximum 10-minute sustained wind speed in excess of 17.2 m s^{-1}) from a tropical depression at 1200 UTC on 10 September 2006 when situated at 16.8ºN, 134.8ºE. Shanshan moved westward and turned toward the north over the sea south of the Southwest Islands on 14 September. Shanshan gradually increased in intensity over the warm sea and passed between Iriomote and Ishigaki Islands at 2100 UTC on 15 September, with a central pressure of 925 hPa and a maximum wind speed in excess of 50 m s^{-1}. During the passage around Ishigaki Island, the eye with the radius of about 40 km was clear and became visible in the satellite image (Fig. 2). Then Ishigaki Island was located in the eye.

Figure 3 shows the time series of surface observation recorded at Ishigaki Island, while figure 4 shows the radar map derived from the weather radar at Ishigaki site. When Shanshan was located over the sea about 300 km south of Ishigaki Island, two outer rainbands (referred to as OB1 and OB2) passed over Ishigaki Island at 1920 UTC on 14 (Fig. 4a) and 0320 UTC on 15 (Fig. 4b), causing heavy precipitation (Fig. 3). Precipitations accompanying outer rainbands were characterized by the heavy convective precipitation with subsequent stratiform precipitation.

After 0900 UTC on 15 September as Shanshan approached close to Ishigaki Island, easterly wind speed gradually increased and relative humidity remained high more than 90 percent (Fig. 3). The weak echo region spreading 150 km north of the center, known as the rain shield (Shimazu 1998), covered over Ishigaki Island (Fig. 4c), causing the stratiform precipitation. In the rain shield, two inner rainbands (referred to as IB1 and IB2) passed over Ishigaki Island (Fig. 4d and e), causing heavy convective precipitation at 1300 and 1600 UTC on 15. After the leaving of IB2, a ring of intense convection surrounding the center, front eye wall (referred to as FEW), started to cover over Ishigaki Island at 1800 UTC.

Although the power failure due to the storm interrupted the weather radar observation after 1900 UTC on 15 (Fig. 4f), precipitation patterns associated with Shanshan were provided by TRMM-TMI observation at 0440UTC on 16 September (Fig. 5). During the passage of FEW over Ishigaki Island for 1800—2040 UTC on 15, heavy convective precipitations and strong easterlies exceeded 45 m s^{-1} were observed (Fig. 3). At 2040—2130 UTC when Ishigaki Island was located in the eye (Fig. 5), no or little precipitation quickly occurred and wind speed weakened with clockwise changes in wind directions (Fig. 3). Clockwise changes in wind directions indicated that Ishigaki Island was to the right of moving direction of Shanshan. The lowest pressure of 924 hPa in the surface pressure was recorded, while surface temperature temporally increased.

Strong westerlies were observed reaching about 50 m s^{-1} following the passing of eye (Fig. 3). The rear eye wall (referred to as REW) caused heaviest precipitation in excess of 10 mm 10-min^{-1}. After the passage of REW, the precipitation accompanying the rain shield ended over Ishigaki Island by 0200 UTC on 16. The wind speeds gradually decreased related to the leaving of Shanshan. As Shanshan moved away from Ishigaki Island, there are no outer rainbands passing over Ishigaki Island.

These meteorological results confirmed that our observations at Ishigaki Island captured the structure of Shanshan during the intensification over the ocean.

3.2 Isotopic features of precipitation and water vapor

From 11 to 18 September 2007, 26 water vapor and 55 precipitation samples were successfully collected. Figure 6 show the time series of δ^{18}O of precipitation and water vapor observed at Ishigaki Island, together with the salinity in the precipitation samples. Although the water vapor sampling was conducted at 6-hour intervals, we irregularly curried out water vapor sampling at 2020—2130 UTC on 15 September during the passage of FEW and eye. The deficiency of liquid nitrogen due to power failure, unfortunately, interrupted the water vapor sampling from 1630 UTC on 16 to 0430 UTC on 17 September.

Isotope values of water vapor had a large range. The isotope ratio of water vapor gradually decreased from -13 per mil at 2230 UTC on 14 to -24 per mil at 1630 UTC on 15 September. The anomalous high isotopes ratio of -13 per mil was appearance at 2100 UTC on 15 September. The d-excess of water vapor increased to 20 per mil at 0430 UTC on 15, and then gradually decreased by 13 per mil at 2100 UTC on 15. After 0430 UTC on 16, the high isotope ratios of water vapor, -6 per mil, remained steady.

On the other hand, isotopic values of precipitation which was corrected for content of sea spray also had a large range. Isotope ratios of precipitation in OB1 and OB2 quickly decreased with significant amplitude more than -5 per mil. From 1030 to 1800 UTC on 15 during the passage of rain shield, precipitation isotope ratios gradual decreased from -7 to -14 per mil. There were discontinuous changes in the precipitation isotope ratios at 1230 and 1530 UTC before the passage of IB1 and IB2. The low d-excess of precipitation, about 8 per mil, remained steady from 1030 to 1500 UTC on 15. During the approach of FEW from 1600 to 1900 UTC on 15, the precipitation isotope ratios increased from -14 to -11 per mil, while the d-excess of precipitation decreased from 10 to 0 per mil. Unfortunately the samples of precipitation in FEW from 1900 to 2200 UTC were

not completely collected. It is remarkable that anomalously high isotope ratios of precipitation occurred in REW at 2200 UTC on 15: the $\delta^{18}O$ values of about -6 per mil were as high as those of OB1 and OB2. After the passage of REW, the isotope ratios in little precipitation decreased down to -13 per mil at 0300 UTC and increased to -7 per mil at 1800 UTC on 16.

In general, as precipitation continues falling, the isotope ratios of precipitation decrease with increasing precipitation totals, which is so-called amount effect (Dansgaard 1964). However, the variability of isotope ratios accompanying Shanshan can not be explained by the amount effect.

4. Discussions

The isotopic ratios in precipitation and water vapor in Shanshan exhibited a distinct and remarkably systematic variation with the radial distance from the TC center. Figure 7 shows the radial profile of $\delta^{18}O$ and d-excess of precipitation and water vapor observed at Ishigaki Island. When an observation site is located on the northern (southern) side of Shanshan and Shanshan approaches (moves away from) Ishigaki Island, the conditions are here referred to as the front (rear) side of Shanshan.

Between 80 and 300 km radius in the front side (referred to as TC's outer region), from the position of OB2 to IB2, an inward decrease in the isotope ratios of water vapor was clearly appearance. The gradient, which was defined as the decreases in the isotope ratios related to the radial distance, was the largest in the area of rain shield between 80 and 160 km radius. The inward decrease in isotope ratios of water vapor was not clear in the rear side of Shanshan. In the contrast, an inward increase in isotope ratios of water vapor was significant around eye and FEW (referred to as TC's inner region). On the other hand, precipitation isotope ratios gradually decreased radially inward in the TC's outer region. In the TC's inner region, the anomalously high of isotope ratios appeared in REW. Furthermore it is found that the d-excess of both precipitation and water vapor tended to decrease inward in the TC's inner and outer regions (referred to as TC's region).

We speculated that the isotopic variation can primarily be attributed to the moisture cycling in the boundary layer. TC-relative winds were divided into two components depending on the wind direction: the tangential wind that flows parallel to curved isobars and its velocity is defined counter-clock wise, and the radial wind that flows toward its center cross the isobars and its velocity is defined positive inward. This analysis was used the 30-minutes averaged surface wind observed at JIRCAS, although the wind was not recorded after 1900 UTC on 15 September.

Figure 8 shows the radial profile of two components of winds. The radial wind increased inward in the TC's outer region, while degreased inward in the TC's inner region. On the other hand, the tangential wind quickly increased inward in the TC's inner region. It suggests that a horizontal convergence was conspicuous in the TC's outer region, whereas a weak horizontal convergence and high winds were appearance in the TC's inner region.

Isotopic observation results show that the inward decrease in isotope ratios of water vapor clearly appeared in the TC's outer region where a horizontal convergence was conspicuous. The largest gradient was in the precipitation region of rain shield when the air passed through regions of precipitation. Furthermore a scatter plot of $\delta^{18}O$ and $\delta^{2}H$ values of water vapor (Fig. 8) shows that, in the front side, the gradient of radial changes in isotope values were not 8 in parallel to the meteoric water line (MWL, Craig, 1961). It means that the radial changes in the isotope ratios are not described by a Reyleigh equation, isotopic fractionation caused by the water changes phases. For these reasons, the inward decrease in isotope ratios of water vapor was mainly caused by the evaporation and diffusive isotope exchange between falling precipitation and converging water vapor in the boundary layer, which is consistent with the previous studies (e.g. Lawrence and Gedzelman 1996). Namely the water vapor, which was isotopically depleted through regions of precipitation, converged in the boundary layer of TC's outer region, causing the inward decreases in water vapor isotope ratios. Since water vapor roughly acts as a source of precipitation, the isotope ratios of precipitation also decreased radially inward to the center.

On the other hand, anomalously high isotope ratio of the water vapor occurred in the TC's inner region where a horizontal convergence was weak and surface wind velocity was high except the local region of eye. In regions of high wind, the evaporation from the sea surface is generally active. Since water vapor that comes directly from the sea surface has high isotopic ratios, the recharge of evaporated water vapor from the sea surface caused the anomalously high values of water vapor isotopes in the TC's inner region. Also the precipitation isotope ratios in the eye wall were isotopically enriched by the source of water vapor with heavy isotopes.

Figure 6c shows the radial profile of salinity in collected precipitation samples. The salinity in precipitation sample quickly increased in the TC's inner region, indicating that sea spray fills the atmosphere due to the high wind over the sea surface (Black et al 1986). Sea spray, having heavy isotope ratios like ocean water, partly evaporates into the air before falling back to the sea surface, causing the water vapor with heavy isotopes. We speculated

that the anomalously high in the water vapor isotope in the TC's inner region was also caused by the recharge of evaporated water vapor from the sea spray filled in the atmosphere (Wang et al. 2001, Gedzelman et al. 2003) as well as the recharge of evaporated water vapor from the sea surface. Due to the limitations of the observational data, quantitative understanding of two kinds of recharge is not clear. Such an examination could be considered for future study using the numerical modeling.

Another remarkable change in isotopic composition during the passage of Shanshan was the inward decreases in the d-excess of both precipitation and water vapor in the TC's region (Fig. 7). The physical process causing the variability in d-excess is mainly evaporation and diffusive water vapor change in subsaturated air, while the production of precipitation from water vapor essentially conserves the d-excess. Since the d-excess of water vapor increases as relative humidity decreases, the higher d-excess of water vapor in the TC's outer region is resulted from a main source region with a lower relative humidity, i.e., environmental moisture surrounding TC. As the air converged to the center in the boundary layer, the d-excess of water vapor decreased inward as water vapor was exchanged with the falling precipitation and evaporated water vapor from the sea surface and sea spray.

It is interesting to note that there are short-term variations in precipitation isotope ratios within individual rainband. Precipitation isotope ratios in OB1 and OB2 quickly decreased with large amplitude. Since heavy isotopes concentrate in liquid and ice during condensation in cloud are preferentially removed from the ambient water vapor by falling precipitation and snow, isotope ratios of precipitation accompanying organized precipitation system decreases in the downwind regions (e.g., Gedzelman and Lawrence 1990, Gedzelman and Arnold 1994). This is one cause for the amount effect (e.g., Dansgaard 1964). In cases of OB1 and OB2, organized precipitation system passed over Ishigaki Island, causing the convective precipitation on the advancing side of subsequent stratiform precipitation. Precipitation isotope ratios, therefore, decreased with increasing precipitation total. During the passage of precipitation region in rain shield, short-term changes in precipitation isotope ratios are very variable. It suggests the complex moisture cycling in the multiple cloud of the TC.

5. Summary

Isotope ratios of precipitation and water vapor during the passage of Typhoon Shanshan were observed at Ishigaki Island. Isotopic observations in which interval is 6 hour and 1-mm amount of precipitation allow a more qualitative understanding of atmospheric moisture cycling of the TC. Observational results are summarized as follows: 1) isotope ratios of both precipitation and water vapor decreased radially inward in the TC's outer region; 2) anomalously high isotope ratios of both precipitation and water vapor appeared in the TC's inner region; 3) the d-excess of both precipitation and water vapor tended to decrease in the TC's region; and 4) the variable short-term changes in precipitation isotope ratios were appearance related to complex moisture cycling in the multiple clouds of the TC.

Figure 10 illustrates the moisture cycling controlling the observed isotopic features with the radial distance from the center. In the TC's outer region where a horizontal convergence is dominant in the boundary layer, the converging water vapor is isotopically depleted due to the evaporation and diffusive isotope exchange between falling precipitation and converging water vapor. A moisture cycling in the TC's outer region is mainly caused by converging water vapor in the boundary layer from environmental moisture surrounding the TC. In the TC's inner region where evaporation is active and a horizontal convergence is weak, water vapor is isotopically enriched by the recharge of evaporated water vapor from the sea surface and sea spray with heavy isotope ratios. It indicates that a major water source for water vapor and precipitation in the TC's inner region is nearby ocean.

These isotopic observational findings are a reflection of significant difference in the major water sources between the TC's inner and outer regions during the intensification of the TC over the ocean. It supports the results of previous numerical studies (e.g., Emanuel 1989). Future work involves developing a mosescale isotopic model to realistically simulate the isotopic features observed in the TC in order to quantitatively discuss the moisture cycling related to the intensification of TCs over the ocean.

References

Black, P. G., R. W. Burpee, N. M. Dorst, and W. L. Adams, 1986: Appearance of the sea surface in tropical cyclones, Wea, Forecasting, 1, 102-107.

Charney, J. G., and A. Eliassen, 1964: On the growth of the hurricane depression. J. Atmos. Sci., 21, 68-75.

Craig, H., 1961: Isotopic variations in meteoric waters, Science 133, 1702-1703.

Dansgaard, W., 1964: Stable isotopes in precipitation. Tellus, 16, 436-468.

Ehhalt, D. H., and H. G. Ostlund, 1970: Deutrium in Harricane Faith, 1966: Preliminary Results. J Geophys Res., 75, 2323-2327.

Emanuel, K. A., 1989: The finite-amplitude nature of tropical cyclogenesis, J. Atmos. Sci., 46, 3431-3456.

Gedzelman, S. D., and R. Arnold, 1994: Modeling the isotopic composition of precipitation. J. Geohys, Res., 99, 10,455-10,571.

Gedzelman, S. D., and J. R. Lawrence, 1990: The isotopic composition of precipitation from two extratropical cyclones, Mon. Wea. Rev., 118, 495-509.

Gedzelman, S. D., J. R. Lawrence, J. Gamache, M. Black, E. Hindman, R. Black, J. Dunion, H. Willoughby, and X. Zhang, 2003: Probing Hurricanes with Stable Isotopes of Rain and Water Vapor, Mon. Wea. Rev., 131, 1111-1127.

Ichyanagi K., K. Yoshimura, and M. D. Yamanaka, 2005: Validation of Changing water origins over Indochina during the withdrawal of the Asian monsoon using stable isotopes, SOLA, 2005, 1, 113-116.

Lawrence, J. R., and S. D. Gedzelman, 1996: Low stable isotope ratios of tropical cyclone rains. Geophys. Res Lett., 23, 527-530.

Lawrence, J. R.,1997: Isotope spikes from tropical cyclones in surface waters: Opportunities in hydrology and paleoclimatology. Chem. Geology, 144 (1998), 153-160.

Lawrence, J. R., S. D. Gedzelman, X. Zhang, and R. Arnold, 1998: Stable isotopes of rain and vapor in 1995 hurricanes. J. Geophys. Res., 103 (D10), 11,381-11,300.

Lawrence, J. R., S. D. Gedzelman, M. Black, and J. Gamache, 2002: Stable isotopes of precipitation collected at 3 km elevation in Hurricane Oliva (1994). J. Atmos. Chem., 41, 67-82.

Lawrence, J. R., and S. D. Gedzelman, 2003: Tropical ice core isotopes: Do they reflect changes in storm activity? Geophys. Res Lett., 30 (1072), doi: 10.1029/2002GL015906.

Lawrence, J. R., S. D. Gedzelman, D. Dexheimer, H. Cho, G. D. Carrie, R. Gasparini, C. R. Anderson, K. P. Bowman, and M. I. Biggerstaff, 2004: Stable isotopes composition of water vapor in the tropics. J. Geophys. Res., 109, doi: 10.1029/2003JD004046.

Merlivat, L. and Jouzel, Z., 1979: Global climatic interpretation of the deuterium oxygen 18 relationship for precipitation, J Geophys, Res, 84, 5029-5033.

Miyake, Y., O. Matsubaya, and O. Nishihara, 1968: An isotopic study of meteoric precipitation, Pap. Meteorol. Geophys., 19, 243-266.

Montgomery, M. T., M. E. Nicholls, T. A. Cram, and A. B. Saunders, 2006: A vertical hot tower route to tropical cyclogenesis. J. Atmos. Sci., 63, 355-386.

Ooyama, K. V., 1964: A dynamical model for the study of tropical cyclone development. Geofis. Int., 4, 187-198.

Ooyama, K. V., 1969: Numerical simulation of the life cycle of tropical cyclones. J. Atmos. Sci., 26, 3-40.

Rotunno, F., and K. Emanuel, 1987: An air-sea interaction theory for tropical cyclones. Part II: Evolutionary study using a nonhydrostatic axisymmetric numerical model. J. Atmos. Sci., 44, 542-561.

Shimazu, Y., 1998: Classification of precipitation systems in mature and early weakening stage of typhoon around Japan. J. Meteor. Soc. Japan, 76, 437–445.

Sugimoto, A., Yanagisawa, N., Naito, D., Fujita, N., Maximov, C. 2002: Importance of permafrost as a source of water for plants in East Siberian Taiga. Ecological Research, 17, 493-503.

Wang, Y., J. D. Kepert, and G. Holland, 2001: On the effect of sea spray evaporation on tropical cyclone boundary layer structure and intensity. Mon. Wea. Rev., 129, 2481-2500.
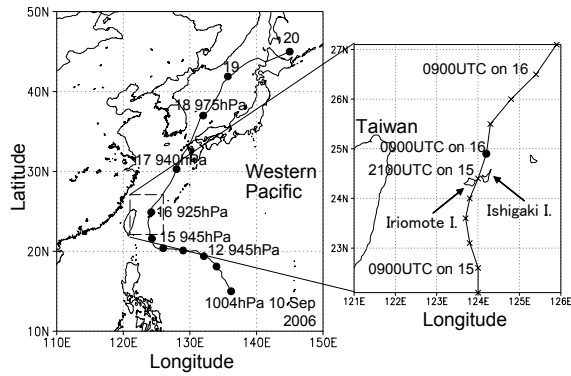
Fig. 1: Track of Shanshan from Best Track data for the period 10—20 September 2006. Closed circles represent positions of Shanshan at 0000 UTC, while crosses represent positions at 0300, 0600, 0900, 1200, 1500, 1800, and 2100 UTC.
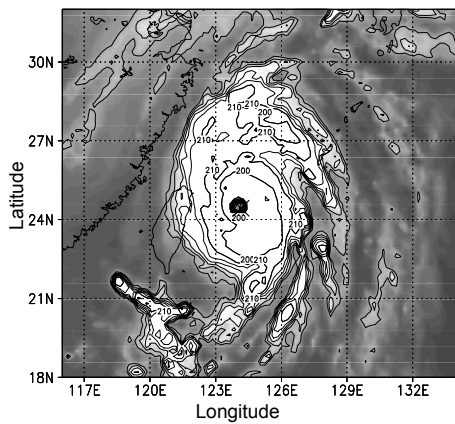
Fig. 2: Equivalent black body temperature (T_{BB}) for 2100 UTC on 15 September 2006. The contour interval is 10 K. A cross represents the position of Ishigaki Island.
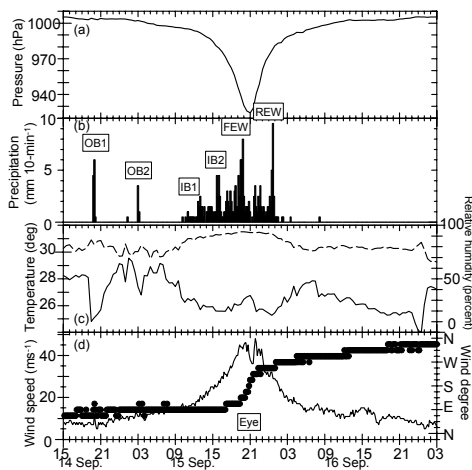
Fig. 3: Record of (a) 30-minutes averaged surface pressure, (b) 10-minute accumulated precipitation, (c) 30-minutes averaged temperature (solid line) and relative humidity (broken line), and (d) 10-minutes averaged wind speed (line) and direction (dots) as observed at Ishigaki Island from 1500 UTC on 14 to 0300 UTC on 17 September 2006.
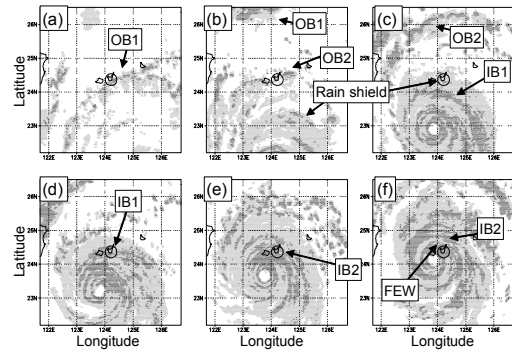
Fig. 4: Radar map of Ishigaki site at (a) 1920 UTC on 14, (b) 0320 UTC, (c) 1100 UTC, (d) 1300 UTC, (e) 1600 UTC, and (f) 1900 UTC on 15 September 2006. Regions of echo intensity of 10-40 mm hour^{-1} are lightly shaded, while regions greater than 40 mm hour^{-1} are heavily shaded. Open circles indicate the positions of Ishigaki Island.
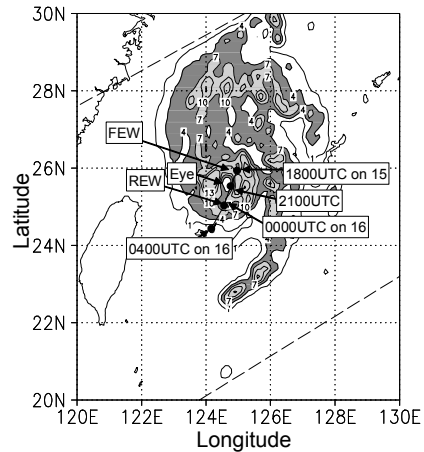
Fig. 5: Surface precipitation map derived from TRMM-TMI at 0440 UTC on 16 September 2006. Regions of echo intensity of 4-7 mm are lightly shaded, while regions greater than 7 mm are heavily shaded. The contour interval is 3 mm. A solid line and cross represent the postions of Ishigaki Island related to the center.

7
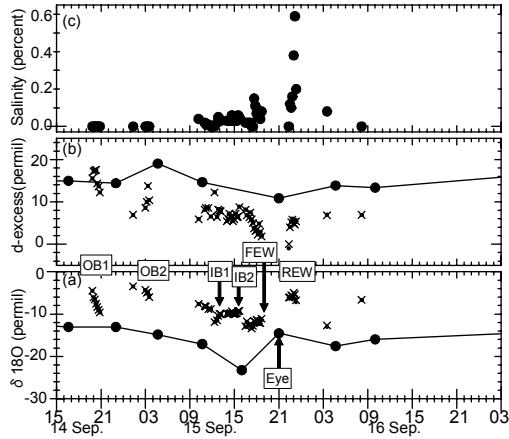
Fig. 6: Record of (a) $\delta^{18}O$, (b) d-excess of precipitation (closed circles and crosses) and water vapor (closed circles with solid line), and (c) salinity in collected precipitation samples from 1500 UTC on 14 to 0300 UTC on 17 September 2006. Crosses indicate observed isotope ratios in precipitation, whereas closed circles indicate isotope ratios which were corrected for content of sea spray.
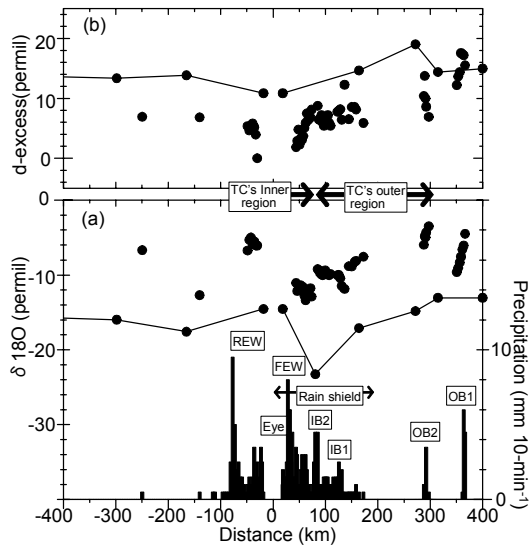
Fig. 7: Radial profile of (a) 10-minuts precipitation (filled bar), $\delta^{18}O$, and (b) d-excess of precipitation (closed circles) and water vapor (closed circles with line). Positive (negative) distance shows the conditions of the front (rear) side of the moving Shanshan.
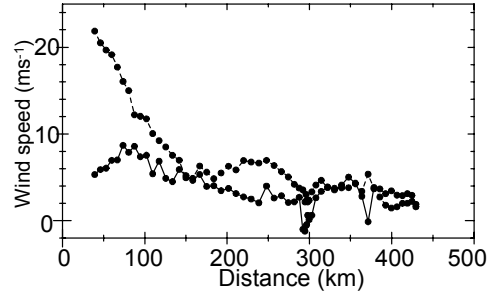
Fig. 8: Radial profile of radial (solid line) and tangential (broken line) winds derived from 30-minute averaged winds observed at Ishigaki Island.
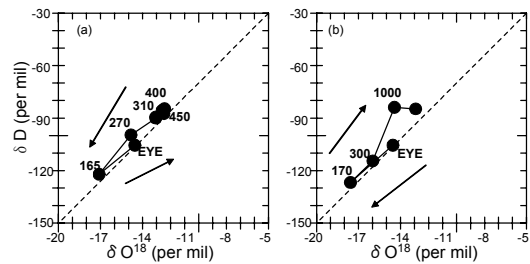
Fig. 9: Scatterplot showing δ^2H and $\delta^{18}O$ for water vapor in (a) front and (b) rear sides. The numbers denote the distance from the center.
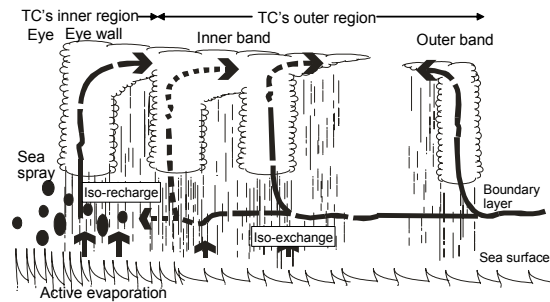
Fig. 10: Schematic cross section of moisture cycling in the tropical cyclone. Solid arrows indicate trajectories of isotopically heavier water vapor, while open arrows indicate trajectories of isotopically lower water vapor. Closed circle indicate the sea spray.